Optical Engineering

OpticalEngineering.SPIEDigitalLibrary.org

Superficial waveguide splitters fabricated by femtosecond laser writing of $LiTaO_3$ crystal

Chen Cheng
Carolina Romero
Javier R. Vázquez de Aldana
Feng Chen

SPIE.

Superficial waveguide splitters fabricated by femtosecond laser writing of $LiTaO_3$ crystal

Chen Cheng,[a] Carolina Romero,[b] Javier R. Vázquez de Aldana,[b] and Feng Chen[a,*]
[a]Shandong University, School of Physics, Jinan 250100, China
[b]Universidad de Salamanca, Laser Microprocessing Group, Departamento Física Aplicada, Salamanca 37008, Spain

Abstract. We report on Y-branch superficial depressed-cladding waveguides fabricated by femtosecond laser writing of $MgO:LiTaO_3$ crystal. The cladding waveguides with a rectangular cross-section are single mode for both transverse electric and transverse magnetic polarization, and show good transmission properties at a telecommunication wavelength of 1.55 μm. Divergence angles as large as 2.6 deg are successfully achieved in the splitters with nearly equalized splitting ratios (1:1). The fabricated shallow structures are excellent photonic elements for optoelectronic applications. [DOI: 10.1117/1.OE.54.6.067113]

Keywords: beam splitters; optical waveguides; femtosecond laser writing; $LiTaO_3$ crystal.

Paper 150447 received Apr. 8, 2015; accepted for publication Jun. 3, 2015; published online Jun. 29, 2015.

1 Introduction

In photonics, based on waveguide technology, various miniature and compact devices, such as beam splitters, directional couplers, and ring resonators, have been widely applied in a number of areas, including modern optical telecommunications, quantum computing, sensing for atmosphere or biology, etc.[1–6] Guided-wave optical devices based on dielectric crystals enable the combination of the features from both the compact geometries and the bulk materials, playing a remarkable role for both passive and active applications; e.g., the $LiNbO_3$-based waveguide devices have been utilized for electro-optic modulation, signal amplification, and frequency conversion.[7–11] Lithium tantalate ($LiTaO_3$), whose features are somehow similar to $LiNbO_3$, exhibits excellent performance for the areas of nonlinear optics, passive infrared sensors, terahertz generation, and electro-optic application.[12,13] It possesses better thermal stability for high-power laser processing and prominent ability for photorefraction, especially for an MgO-doped crystal, compared with the commonly used $LiNbO_3$.[14–17] Although a number of techniques have been developed to produce waveguides in $LiTaO_3$ crystal as well as other dielectric crystals, the fabrication of guiding structures for such a purpose entails considerable difficulty due to the complexity of crystalline structures, bulk chemical/physical features, and the limitations of each technique applied to different materials.[18–22] Direct femtosecond laser writing has recently become a powerful technique to realize three-dimensional (3-D) micromachining of diverse materials for a broad range of applications.[23–25] High-intensity femtosecond laser pulses allow the micromodification of the material matrix with an extreme precision through strong-field ionization processes. In particular, it has become a unique technique to fabricate waveguides in optical materials since 1996.[26] In most glasses, intense femtosecond laser pulses usually induce positive changes of the refractive index ($\Delta n > 0$) inside the laser-irradiated volumes. This feature enables direct 3-D microfabrication of various optical devices. Significantly different, femtosecond lasers typically induce negative index changes ($\Delta n < 0$) at the irradiated tracks of dielectric crystals.[8,10] In addition, a depressed cladding waveguide can be fabricated by femtosecond laser writing as well, whose guiding core (undamaged) is normally surrounded by a number of laser-induced low-index tracks. In a 3-D view, the cladding waveguides are similar to photonic tubes, with circular or rectangular cross-sections and arbitrary diameters (typically from 20 to 200 μm)[10] In photonics, the Y-branch waveguides are essential elements for beam splitting or interferometers, which are extensively applied in various areas of electro-optical modulations, optical communications, or integrated optical chips.[25,27] In many optoelectronic applications, the waveguides or photonic circuits are required to be near the surface of the host material. However, most of the reported waveguides fabricated by femtosecond laser irradiation were buried at a certain depth inside the wafers. In this work, we report on the superficial Y-branch waveguides with rectangular cross-sections by the femtosecond laser writing of a z-cut $LiTaO_3$ crystal wafer. The waveguides support nearly single-mode guidance at the telecommunication wavelength of 1.55 μm and show splitting ratios of $\sim 1:1$.

2 Experiments Details

The z-cut $LiTaO_3$ crystal wafer was cut to the dimensions of $7(x) \times 5(y) \times 3(z)$ mm^3 and was optically polished. The laser writing of the structures was implemented by using the facility at University of Salamanca, Spain. An amplified Ti:Sapphire femtosecond laser (Spitfire, Spectra Physics) that delivered linearly polarized pulses with a temporal duration of 120 fs, a central wavelength of 795 nm, and operating at a repetition rate of 1 kHz was used as the laser source. The beam was focused by a 20× microscope objective and the pulse energy was reduced to 0.4 μJ (after the objective) by using a set of $\lambda/2$ waveplate and linear polarizing cube and

*Address all correspondence to: Feng Chen, E-mail: drfchen@sdu.edu.cn

0091-3286 /2015/$25.00 © 2015 SPIE

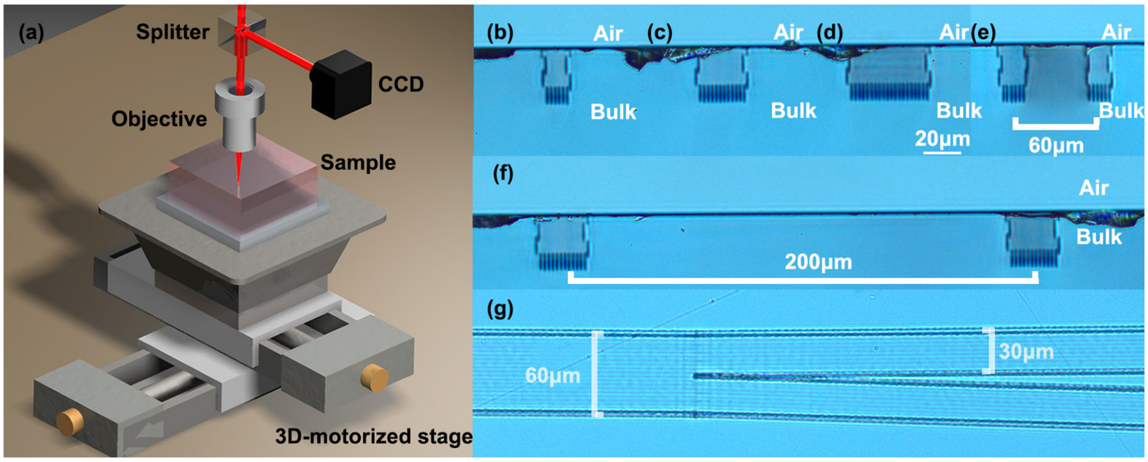

Fig. 1 (a) Schematic plot of the fabrication process with the femtosecond laser. (b), (c), and (d) Microphotograph of the cross-sections of $LiTaO_3$ waveguides with sections of 15, 30, and 60 μm.

a calibrated neutral density filter. The laser irradiation was controlled with a mechanical shutter. The sample was placed on an XYZ micropositioning stage that allowed scanning the sample at constant velocity (0.5 mm/s) along the y direction while irradiating the sample from the surface of 7×5 mm^2 with the femtosecond pulses. Under these conditions, the laser irradiation produced a damage line in the crystal. Many parallel damage lines were inscribed at certain depths of the sample, with a lateral separation of 3 μm, in order to obtain the desired rectangular shape of the waveguide. Figure 1(a) shows the schematic plot of the waveguide fabrication process.

Both rectangular straight waveguides and Y-branch structures were inscribed following this procedure. The design of the Y-branch structures consists of a straight bus waveguide (w width) that is split into two divergent identical waveguides ($w/2$ width). An angle (from 0.8 to 2.6 deg) is fixed between the two split waveguides, ensuring a distance between the two exiting ports of the Y-branch at the end-face as large as 200 μm. For steadily exciting the guiding mode, a 2.52-mm-long straight bus waveguide and 4.48-mm-long split channels are carefully chosen. The microphotograph of the straight bus waveguides with widths of 15, 30, and 60 μm [Figs. 1(b)–1(d)] were imaged by an optical microscope (Axio Imager, Carl Zeiss) operating in transmission mode. Table 1 shows all the details of the fabricated straight bus and Y-branch structure waveguides, including widths of the input and output channels, measured separations at the output face, and the number of the corresponding microphotograph.

Table 1 List of fabricated waveguides.

Number	Type	Width (input/output)	Branches separation	Figure
1	Straight bus	15 μm	None	Fig. 1(b)
2	Straight bus	30 μm	None	Fig. 1(c)
3	Straight bus	60 μm	None	Fig. 1(d)
4	Y-branch	30 μm/15 μm	60 μm	Fig. 1(e)
5	Y-branch	30 μm/15 μm	200 μm	Not shown
6	Y-branch	60 μm/30 μm	75 μm	Not shown
7	Y-branch	60 μm/30 μm	210 μm	Fig. 1(f)

Figure 1(g) depicts the detail of the joint between a straight bus waveguide and two split waveguides, with widths of 60 μm (input) and 30 μm (output), which corresponds to the Y-branch structure waveguides shown in Fig. 1(f).

To investigate the near-field modal distributions of the straight bus and Y-branch structure waveguides, a typical end-face coupling system was employed. The arrangement of the experimental components is shown in Fig. 2. A 1550-nm fiber super luminescent LED light source with random polarization, using a fiber collimator to set light off the fiber to the free space, was coupled into one end-face of the $LiTaO_3$ sample by an objective lens. Another microscope objective lens was used as the out-coupler through which the transmitted light was collected and imaged by a CCD camera. Based on the arrangement, the N.A. of the waveguide was measured in order to get the maximum value of refractive index change of the straight bus waveguides by rotating a large square glass to adjust the position of the incident coupling light. The propagation losses of the structures were estimated and determined by directly measuring the powers of the injected and the output light using a 1064-nm solid-state laser source.

3 Results and Discussion

Figures 3(a) to 3(c) depict the measured near-field modal distributions of the straight bus waveguides with widths of 15, 30, and 60 μm at 1550 nm, respectively (as well as waveguides 1–3 in Table 1), with dash lines labeling the air-crystal

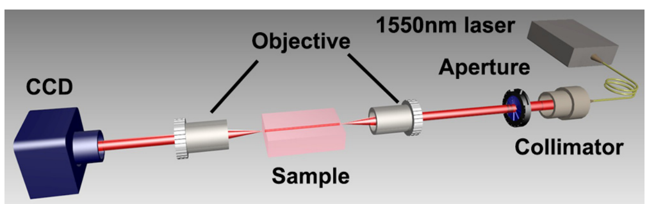

Fig. 2 Arrangement of the experimental components for modal characterization.

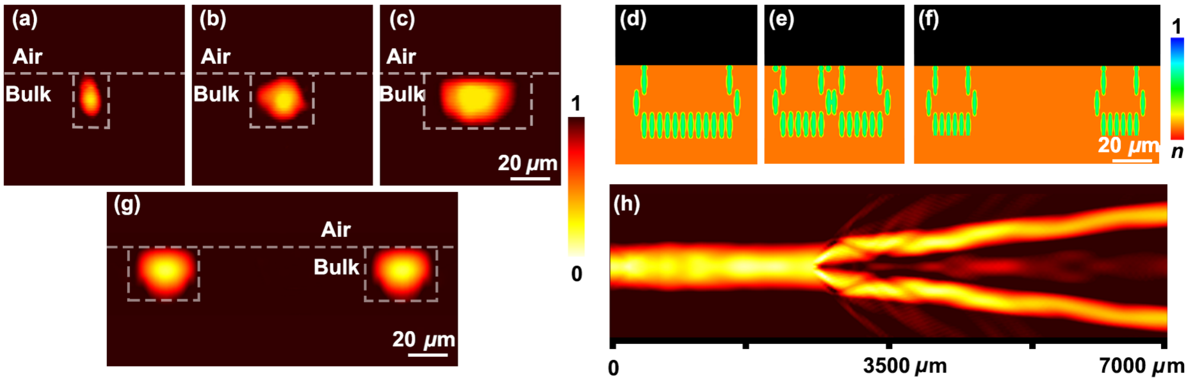

Fig. 3 Measured modal profiles (intensity distribution) of straight bus waveguides with widths (a) 15 μm, (b) 30 μm, and (c) 60 μm at 1550 nm. Simulated refractive index distribution at the cross-section of (d) input port, (e) joint, and (f) output port, as well as (g) simulated modal profiles and (h) propagation, through the Y-branch (30 μm/15 μm input/output widths) with output branch separation of 60 μm.

surface and waveguide cores. As one can see, the channel waveguides supported nearly single-mode guiding. We numerically calculate the modal profiles of the waveguides based on the estimation of the laser-induced refractive index changes. In order to get the refractive index change of the waveguide, the N.A. of the waveguide was estimated using the method introduced by Siebenmorgen et al.[28] By assuming a step-index profile of femtosecond laser modification, the refractive index modification could be roughly approximated by using the equation

$$\Delta n_{o,e} \approx \frac{\sin^2 \theta m}{2n_{o,e}}, \tag{1}$$

where θ_m is the maximum incident angular deflection at which no transmitted power change occurs ($\theta_m = 3.5$ deg with a difference of 0.3 deg between both polarizations). The estimated index modification was then $\Delta n_{o,e} \approx 1 \times 10^{-3}$ for the laser-written $LiTaO_3$ waveguides. By difference of refractive indices, the refractive index distributions at different positions are simulated (input port, joint, and output port, Figs. 3(d) to 3(f)] by the prototype of the Y-branch (30 μm/15 μm input/output widths) with an output branch separation of 60 μm as an example.

By setting the refractive index distribution, the propagation through Y-branch structures were simulated by the FD-BPM algorithm (Rsoft® Beam PROP) using the data of the calculated refractive index modification. In Figs. 3(g) and 3(h), we show the results of modal profiles and propagation for waveguide 5 in Table 1 (30 μm-input/15 μm-output with a branch separation of 60 μm).

The measured near-field modal profiles of the Y-branch structure waveguides 4 to 7 are depicted in Figs. 4(a) to 4(d), respectively. The splitting ratios were estimated by integrating the measured intensity distributions corresponding to each output port, and we obtained 1.19:1 (4), 1.11:1 (5), 1.06:1 (6), and 1.08:1 (7).

As an essential factor in the performance of the waveguides, propagation losses of the waveguides in $LiTaO_3$ crystal were estimated. The total losses of the straight bus waveguides (including propagation losses and coupling losses) were measured by an end-face coupling system at 1064 nm. The values of waveguides 1 to 3 with transverse electric (TE) [transverse magnetic (TM)] polarization were −4.39, −2.43, and −2.25 dB (−4.65, −3.45, and −3.01 dB), respectively.

The mismatch of the launched Gaussian beam with the modal profiles of the waveguide can be calculated by an overlap integral between both field profiles. Here, it is assumed that the incident field is Gaussian (E_G) and the waveguide mode is E_P, resulting in a mismatch coefficient C that can be expressed as[29,30]

$$C = \frac{1}{2}\left(\frac{\varepsilon 0}{\mu 0}\right) \int_S E_G * E_P \mathrm{d}S. \tag{2}$$

The losses, α, of the modal mismatch can be obtained by the following equation:

$$\alpha = -10 \log(|C|^2). \tag{3}$$

With an assumption of a 20-μm-diameter input Gaussian field E_G (estimated by experimental experience), the value can be calculated by the FD-BPM algorithm (Rsoft® Beam PROP) (∼ − 3, −1.1, and −0.9 dB for 1, 2, and 3). In consideration of the Fresnel reflection, it gives rise to a loss (−0.61 dB) at each waveguide–air interface. Along those lines, for the 7-mm-long straight bus waveguides

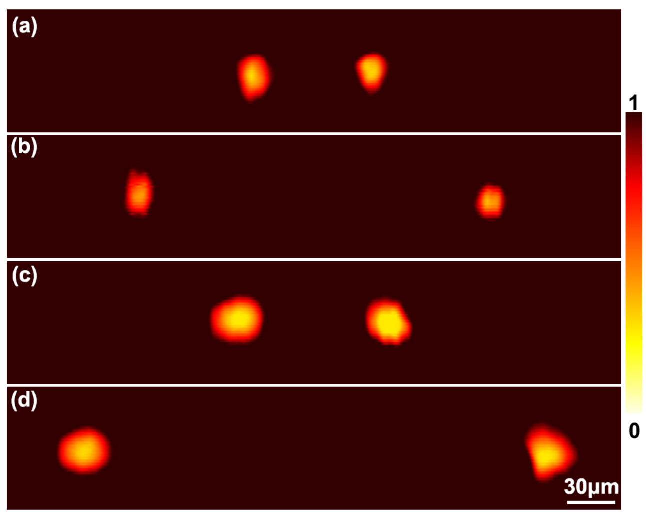

Fig. 4 (a) to (d) Measured near-field modal profiles of the Y-branch structure waveguides 4 to 7.

1 to 3, the propagation losses are determined as low as ~0.24, 0.13, and 0.12 dB/cm (0.61, 1.93, and 1.27 dB/cm) in the TE (TM) polarized orientation, respectively. Compared with other techniques for fabricating superficial waveguiding strucures in $LiTaO_3$ crystals, e.g., Ar^{8+} ion irradiation for a planar waveguide with a propagation loss of ~2.8 dB/cm or proton exchange for Y-branch $LiTaO_3$ waveguides of 4.0 dB/cm loss, the femtosecond laser writing is more advantagous for low-loss waveguide fabrication.[31,32]

4 Summary

In summary, we have reported Y-branch structure waveguides in $LiTaO_3$ crystal fabricated by the femtosecond laser writing with different widths and splitting angles. The guiding properties and propagation at 1550 nm were investigated, showing nearly single-mode guidance in straight bus waveguides and Y-branch structures. The good performances obtained, without polarization sensitivity, suggest that the produced Y-branch structure waveguides in the $LiTaO_3$ crystal are potential candidates in optical communication and electro-optical applications.

Acknowledgments

This work was supported by the National Natural Science Foundation of China (Grant No. U1332121) and Ministerio de Economía y Competitividad under Project FIS2013-44174-P, Spain.

References

1. G. Lifante, *Integrated Photonics: Fundamentals*, Wiley, England (2003).
2. F. Chen and J. R. V. de Aldana, "Optical waveguides in crystalline dielectric materials produced by femtosecond-laser micromachining," *Laser Photon. Rev.* **8**(2), 251–275 (2014).
3. E. J. Murphy, *Integrated Optical Circuits and Components*, Marcel Dekker, New York (1999).
4. D. G. Rabus, *Integrated Ring Resonators*, Springer, Berlin (2007).
5. W. Fritzsche and J. Popp, *Optical Nano-and Microsystems for Bioanalytics*, Springer Science & Business, Media, Berlin, Heidelberg (2012).
6. C. Grivas, "Optically pumped planar waveguide lasers, part I: fundamentals and fabrication techniques," *Prog. Quantum Electron.* **35**(6), 159–239 (2011).
7. J. Burghoff, S. Nolte, and A. Tunnermann, "Origins of waveguiding in femtosecond laer structured $LiNbO_3$," *Appl. Phys. A* **89**(1), 127–132 (2007).
8. A. Okhrmchuk et al., "Low loss depressed cladding waveguide inscribed in YAG:Nd single crystal by femtosecond laser pulses," *Opt. Express* **20**(4), 3832–3843 (2012).
9. D. Jaque, E. Cantelar, and G. Lifante, "Lattice micro-modifications induced by Zn diffusion in $Nd:LiNbO_3$ channel waveguides probed by Nd^{3+} confocal micro-luminescence," *Appl. Phys. B* **88**(2), 201–204 (2007).
10. R. Y. He et al., "Femtosecond laser micromachining of lithium niobate depressed cladding waveguides," *Opt. Mater. Express* **3**(9), 1378–1384 (2013).
11. Y. Tan, J. R. V. de Aldana, and F. Chen, "Femtosecond laser-written lithium niobate waveguide laser operating at 1085 nm," *Opt. Eng.* **53**(10), 107109 (2014).
12. N. E. Yu et al., "Simultaneous forward and backward terahertz generations in periodically poled stoichiometric $LiTaO_3$ crystal using femtosecond pulses," *Appl. Phys. Lett.* **93**(4), 041104 (2008).
13. P. Baldi et al., "Proton exchanged waveguides in $LiNbO_3$ and $LiTaO_3$ for integrated lasers and nonlinear frequency converters," *Opt. Eng.* **37**(4), 1193–1202 (1998).
14. G. Y. Liu et al., "Optical waveguides in $LiTaO_3$ crystals fabricated by swift C^{5+} ion irradiation," *Nucl. Instrum. Methods Phys. Res. B* **325**, 43–46 (2014).
15. M. M. Xu et al., "Femtosecond laser micromachined optical waveguides in $LiTaO_3$ crystal," *Phys. Status Solidi RRL* **7**(11), 1014–1017 (2013).
16. K. M. Wang et al., "Waveguide formation in $LiTaO_3$ and LiB_3O_5 by keV hydrogen ion implantation," *Opt. Commun.* **196**(1–6), 215–219 (2001).
17. D. W. Ward, E. R. Statz, and K. A. Nelson, "Fabrication of polaritonic structures in $LiNbO_3$ and $LiTaO_3$ using femtosecond laser machining," *Appl. Phys. A* **86**(1), 49–54 (2007).
18. B. McMillen et al., "Waveguiding and nonlinear optical properties of three-dimensional waveguides in $LiTaO_3$ written by high-repetition rate ultrafast laser," *Appl. Phys. Lett.* **93**(11), 111106 (2008).
19. R. R. Gattass and E. Mazur, "Femtosecond laser micromachining in transparent materials," *Nat. Photonics* **2**(4), 219–225 (2008).
20. J. I. Mackenzie, "Dielectric solid-state planar waveguide lasers: a review," *IEEE J. Sel. Topics Quantum Electron.* **13**(3), 626–637 (2007).
21. F. Chen, "Construction of two-dimensional waveguides in insulating optical materials by means of ion beam implantation for photonic applications: fabrication methods and research progress," *Crit. Rev. Solid State Mater. Sci.* **33**(3–4), 165–182 (2008).
22. Y. Tan, F. Chen, and H. Zhang, "Optical ridge waveguides in SBN crystal produced by low-dose carbon ion implantation followed by a sputter etching technique," *Opt. Express* **15**(25), 16696–16701 (2007).
23. A. Rodenas and A. K. Kar, "High-contrast step-index waveguides in borate nonlinear laser crystals by 3D laser writing," *Opt. Express* **19**(18), 17820–17833 (2011).
24. A. Benayas et al., "Microstructuring of Nd:YAG crystals by proton-beam writing," *Opt. Lett.* **35**(23), 3898–3900 (2010).
25. Y. Jia et al., "Efficient lasing in continuous wave and graphene Q-switched regimes from Nd:YAG ridge waveguides produced by combination of swift heavy ion irradiation and femtosecond laser ablation," *Opt. Express* **22**(11), 12900–12908 (2014).
26. K. M. Davis et al., "Writing waveguides in glass with a femtosecond laser," *Opt. Lett.* **21**, 1729–1731 (1996).
27. R. Y. He et al., "Three-dimensional dielectric crystalline waveguide beam splitters in mid-infrared band by direct femtosecond laser writing," *Opt. Express* **22**(25), 31293–31298 (2014).
28. J. Siebenmorgen et al., "Femtosecond laser written stress-induced $Nd:Y_3Al_5O_{12}$ (Nd:YAG) channel waveguide laser," *Appl. Phys. B* **97**(2), 251–255 (2009).
29. D. Marcuse, *Theory of Dielectric Optical Waveguides*, Academic, New York (1974).
30. RSoft Design Group, "BeamPROP," 2007, http://www.rsoftdesign.com.
31. P. Liu et al., "Visible and near-infrared waveguide properties in $LiTaO_3$ crystal produced by swift Ar^{8+} ion irradiation," *Appl. Phys. B* **108**(3), 675–681 (2012).
32. W. K. Burns, M. M. W. Howerton, and R. P. Moeller, "Performance and modeling of proton exchanged $LiTaO_3$ branching modulators," *J. Lightwave Technol.* **10**(10), 1403–1408 (1992).

Chen Cheng received his BS degree from Shandong Normal University, Jinan, China, in 2013. He is currently working toward his PhD at Shandong University, Jinan, China. His current research interests include fabrication of optical waveguides in optical crystals by using femtosecond laser writing.

Carolina Romero received the degrees of Bachelor of Science in 2006 from the University of Santiago de Compostela, Spain, and PhD in 2012 from the University of Salamanca, Spain. She is currently a specialized technician at the Laser Microprocessing Group of the University of Salamanca. Her research is concentrated on ultrafast nonlinear optics and laser microprocessing.

Javier R. Vázquez de Aldana received his Bachelor of Science degree in 1997 and his PhD in 2001 from the University of Salamanca, Spain. He is currently an associate professor of the Science Faculty, University of Salamanca, Spain. His research activity is focused on the interaction of intense femtosecond pulses with materials and its application to fabrication of photonic devices. He is a member of the Laser Microprocessing Research Group and is also a technical and scientific advisor of the Laser Facility at the University of Salamanca.

Feng Chen is a professor at Shandong University, China. He received his PhD from Shandong University in 2002. He was with Clausthal University of Technology, Germany, from 2003 to 2005, as a Humboldt research fellow. He has published about 200 papers in peer-reviewed journals. He is a fellow of the Institute of Physics, United Kingdom, a senior member of OSA, and a member of SPIE. He also serves as an associate editor of *Optical Engineering*.